

## Note: Self-characterizing ultrafast pulse shaper for rapid pulse switching

Brett J. Pearson<sup>1,a)</sup> and Thomas C. Weinacht<sup>2</sup>

<sup>1</sup>*Department of Physics and Astronomy, Dickinson College, Carlisle, Pennsylvania 17013-2896, USA*

<sup>2</sup>*Department of Physics and Astronomy, Stony Brook University, Stony Brook, New York 11794-3800, USA*

(Received 23 February 2012; accepted 13 April 2012; published online 26 April 2012)

We use a high-efficiency acousto-optic modulator at the input to a two-dimensional Fourier-domain pulse shaper to achieve built-in characterization of the shaped output pulses. The acousto-optic modulator directs the beam to different vertical positions on a two-dimensional spatial light modulator, each of which can contain a different pulse shape. The undiffracted portion of the light serves as a reference beam for characterizing the shaped pulse via spectral interferometry. Pulse switching rates of 100 kHz can be achieved, making the device especially useful for quantum-control spectroscopy. © 2012 American Institute of Physics. [<http://dx.doi.org/10.1063/1.4708618>]

Ultrafast lasers are powerful tools for observing and controlling molecular systems relevant for biochemistry. The broad spectral bandwidth associated with these pulses can cover several electronic and vibrational states in a molecule, permitting excitation of both electronic and nuclear degrees of freedom. This has proven extremely useful in applications such as multiphoton microscopy<sup>1</sup> and coherent anti-Stokes Raman scattering spectroscopy.<sup>2,3</sup> Combined with optical pulse shaping devices, ultrafast lasers drive the growing field of quantum control spectroscopy<sup>4-6</sup> that can retrieve high-resolution frequency information across broad spectral regions.

Two primary methods exist for encoding the phase and amplitude in a programmable manner with a Fourier-domain, ultrafast optical pulse shaper: liquid crystal displays (LCD), and acousto-optic modulators (AOM).<sup>7</sup> While both approaches have their advantages and disadvantages, their ranges of useful repetition rates are very different. AOMs utilize a traveling acoustic wave, which must leave the interaction region before the next optical pulse arrives. Since this wave travels at acoustic velocities, it requires many microseconds of time between laser pulses. So although an AOM-based device can switch the shape every pulse, it can only be used with lasers with repetition rates of approximately 100 kHz.

Unlike AOMs, LCDs are quasi-static devices, holding their voltage (and hence pulse shape) indefinitely. This allows them to support shaping of high-repetition rate laser oscillators (hundreds of MHz to GHz), giving them an advantage in achieving high signal-to-noise and making them particularly desirable for microscopy applications. However, the capacitance of typical LCDs means that changing the voltage requires time, and the maximum switch rate when changing pulses is typically tens of hertz. So although LCDs may be used with higher repetition-rate lasers, when one changes pulse shapes a significant number of laser shots are lost. This is particularly problematic in many control experiments, where either a large number of pulse shapes are evaluated (e.g., in feedback approaches), or when one rapidly

switches between a limited number of different pulse shapes (e.g., control microscopy).

In order to address the intrinsically slow update rate of LCD-based shapers, previous work used a galvanometer to rapidly switch between pulses on a two-dimensional LCD, where the second dimension was used to write a number of different pulse shapes.<sup>8</sup> By rapidly scanning the laser beam across this dimension using a galvanometer, one can increase the effective update rate substantially. This type of device has already been used to improve the switching speed in experiments studying dynamic biological samples.<sup>9</sup>

In this work, we present a device using all-electronic switching (no moving parts) that achieves self-characterization of the shaped beam by utilizing an AOM as the beam steering element. The undiffracted portion of the light serves as a reference beam for characterizing the shaped pulse via spectral interferometry,<sup>10</sup> and pulse switching rates of 100 kHz can be achieved. We expect the device to be useful in a broad range of quantum-control and nonlinear spectroscopy experiments (e.g., 2D spectroscopy via pulse shaping<sup>6</sup>).

The experimental apparatus is shown in Fig. 1. The input beam from a Ti:Saph oscillator is directed into a high-efficiency AOM oriented such that the diffracted beam is deflected in the vertical direction. The AOM (Isomet 1205C-x-804B) can achieve 85% diffraction efficiency near 800 nm using a 90 MHz acoustic wave. The Bragg region in the AOM is imaged using a one-to-one telescope onto a diffraction grating, after which both the diffracted and undiffracted beams traverse a standard 4-f, Fourier-domain pulse shaper with a two-dimensional LCD in the Fourier plane. The two beams reflect off the LCD and retrace their respective paths through the device. The LCD is a Holoeye LC-R 2500, which is 1024 pixels wide by 768 pixels high, with a pixel pitch of 19  $\mu\text{m}$  and a fill factor of 93%.<sup>11</sup>

The overall efficiency of the device when optimizing for the diffracted beam is approximately 45%, a figure that takes into account two diffractions from the AOM (85% each), two diffractions from the grating (93% each), and the reflection from the LCD (75%). Losses from the anti-reflection-coated lenses are minimal. When performing spectral interferometry, the amplitude of the voltage wave applied to the AOM is

<sup>a)</sup> Author to whom correspondence should be addressed. Electronic mail: [pearsonb@dickinson.edu](mailto:pearsonb@dickinson.edu).

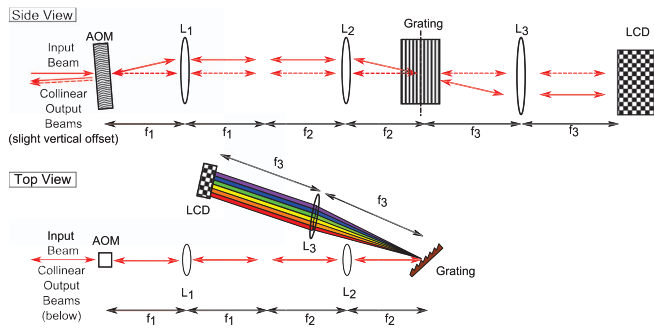


FIG. 1. Layout of two-dimensional pulse shaper with both side (top panel) and overhead (bottom panel) view. For clarity, the side view is shown “unfolded,” with the grating acting in transmission. Lenses and their respective focal lengths are labeled with  $L$  and  $f$  (in our arrangement  $f_1 = f_2 = 150$  mm,  $f_3 = 250$  mm).

set to maximize the interference contrast of the diffracted and undiffracted beams.

By writing a phase profile only to the portion of the LCD with the diffracted beam, the two beams become our “shaped” and “reference” pulses. Upon return to the AOM, the shaped output beam once again undergoes diffraction, as it again satisfies the Bragg condition. Furthermore, any spectral dispersion from the AOM, or variation of diffraction angle with wavelength, in the diffracted beam due to the large fractional optical bandwidth of femtosecond pulses is automatically removed with the second diffraction on the return trip. The shaped output beam overlaps with the reference beam that has passed through the device undiffracted. By applying a slight vertical tilt in the pulse shaper, the beams are picked-off and detected by a high-resolution spectrometer for self-characterization using spectral interferometry. When the shaped beam is used for experiments, changing the frequency of the AOM acoustic wave with one or more voltage-controlled oscillators (VCOs) allows for scanning the diffracted beam across a vertical range on the LCD. By programming distinct pulse shapes at different vertical positions, we take advantage of the increased update rate that comes with a two-dimensional LCD.

We first consider the ability of the device to self-characterize the shaped output pulses. Spectral interferometry, which uses the spectrally resolved interference between two beams to measure their frequency-dependent relative phase,<sup>10</sup> requires the beams to be phase-locked so that the interference fringes are stable (unless done on a single laser shot). Since the two beams in our device encounter identical optical elements, no significant efforts are required to overcome phase instability due to vibrations. However, the shaped pulse acquires an additional phase upon Bragg diffraction, with the amount dependent on the acoustic phase at the time the beam passes through the AOM. For the interference fringes to be stable over a typical spectrometer detection window of a few milliseconds, the acoustic wave must impart the same phase to each optical pulse. This can be accomplished by generating the acoustic wave directly from the oscillator pulse train with a photodiode and low-pass filter, automatically locking the frequency of the acoustic wave to the repetition rate of the laser.

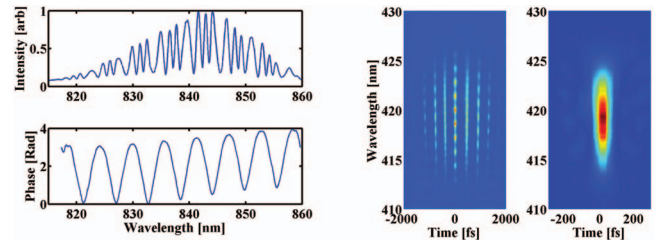


FIG. 2. Left: Raw spectral interferometry signal (top) and reconstructed phase (bottom) for the sine-phase shaped pulse. The phase is retrieved using a variation of the technique discussed in Ref. 10. Middle: SHG-FROG trace of the same sine-phase shaped pulse. Right: SHG-FROG trace of the reference pulse (note the different time axis).

The upper left panel in Fig. 2 shows the raw spectral interferometry signal when a sinusoidal phase is programmed onto the shaped pulse. We have introduced a slight delay between the reference and shaped pulses by means of a glass slide in order to more easily perform the inversion of the interferogram to extract the phase (we use a variation of the technique discussed in Ref. 10). This delay manifests itself in the fast oscillations, while the applied sinusoidal phase appears as the slower variations. The lower left panel plots the retrieved phase from this interferogram, which clearly shows a sinusoidal-like oscillatory pattern with approximately  $\pi$  radians of phase. The slight non-sinusoidal shape of the troughs is due to the fact that the actual phase on the LCD is not quite linear with applied voltage (this can be easily corrected using the voltage-to-phase calibration of the LCD).

Since spectral interferometry only measures the *relative* phase between the shaped and reference pulse, it is important to characterize the reference beam independently. Figure 2 (right panel) shows the second-harmonic generation, frequency-resolved optical gating (SHG-FROG; Ref. 12) trace of the reference pulse. The measured pulse is near the bandwidth limit, implying there is little residual phase on the reference and that the extracted phase is an accurate reflection of the spectral phase on the shaped pulse. This reference pulse duration was achieved after adjusting the grating-lens ( $L_3$ ) separation slightly away from the 4- $f$  configuration to compensate for residual second-order material dispersion of the laser output coupler, lenses, and AOM.

Results from spectral interferometry can be independently confirmed by measuring a FROG of the shaped output pulse. Figure 2 (middle panel) shows a SHG-FROG trace for the shaped pulse with the sinusoidal spectral phase discussed above. In this particular case, we applied a sinusoidal phase with a period of approximately 2.4 THz, which should result in a temporal profile of peaks separated by just over 400 fs (in good agreement with the measured pulse). As with all 4- $f$  shaping devices, limits on the pulses that can be produced are set by the bandwidth of the laser and the resolution of the shaper. In our current configuration with 17 THz of bandwidth across the full width of the LCD and a focal spot size of approximately  $100 \mu\text{m}$ , we can create pulses with temporal durations out to 4 ps whose fastest features are 50 fs.

We next consider the performance of the device for rapidly switching between different pulse shapes. In order

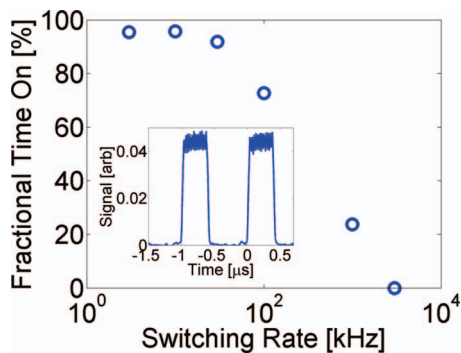


FIG. 3. Maximum switching performance as measured by the percentage of time the shaped beam lies at the correct position on the LCD mask. Inset: Example oscilloscope trace used for calculating the fractional time the device is on.

to change vertical positions on the LCD, and therefore pulse shapes, one needs to vary the frequency of the rf-wave driving the AOM; we examine three separate approaches below. The first method uses a signal generator to adjust the control voltage of a single VCO. This approach is ideal for sweeping through multiple pulse shapes or for relatively low switch rates. The slow rate of our particular VCO (Mini-Circuits ZOS-150) limited us to switch rates of approximately 10 kHz; using a faster VCO would allow for faster switching.

A second approach we tested utilized two independent VCOs running at fixed frequencies of 65 MHz and 95 MHz. The two VCO outputs were fed into two separate rf-frequency mixers (Mini-Circuits ZLW-3), where they were mixed with identical square waves  $180^\circ$  out of phase. Combining the two mixer outputs results in an rf-wave that rapidly switches between two fixed frequencies. Although this approach would quickly become complicated when scaling to many pulse shapes, it is ideally suited for achieving the highest switch rates possible. The results of this experiment are summarized in Fig. 3, which shows the percentage of time the beam spends at the correct position on the LCD (“fractional time on”) as a function of switch rate. The operation is fundamentally limited by the transit time of the acoustic wave across the laser beam profile in the AOM, as pulses that arrive as the change in the acoustic wave transits the beam spot are effectively lost. For a spot size of a couple millimeters, the transit time is approximately 500 ns, which corresponds

to a theoretical maximum switching rate of 2 MHz. We find that our configuration works well up to 100 kHz, with the performance degrading at rates above a couple hundred kHz. The inset of Fig. 3 shows an example of an oscilloscope trace used to calculate the switching performance. The trace plots the signal from a photodetector looking at the output of the pulse shaper when one of the two shaped beams has been blocked. A final approach for switching between pulse shapes, which we considered but did not explicitly evaluate, is to use a programmable arbitrary waveform generator to directly synthesize the rf-wave driving the AOM. This approach combines the ability to sweep through multiple pulse shapes while maintaining rapid switching capabilities.

In summary, we have demonstrated an ultrafast optical pulse shaper featuring all-electronic switching and the ability to self-characterize the shaped output pulses using spectral interferometry. The device can be used with high repetition-rate laser oscillators and can rapidly switch between different pulse shapes at rates up to 100 kHz. We expect the device to be applicable in quantum-control spectroscopy experiments where fast switch rates and high signal-to-noise are required.

We gratefully acknowledge support from the National Science Foundation under Grant No. 0854922 and Dickinson College. We also thank Martin G. Cohen at Stony Brook University for assistance with the AOM and associated electronics.

- <sup>1</sup>W. R. Zipfel, R. M. Williams, and W. W. Webb, *Nat. Biotechnol.* **21**, 1369 (2003).
- <sup>2</sup>B. von Vacano and M. Motzkus, *Phys. Chem. Chem. Phys.* **10**, 681 (2008).
- <sup>3</sup>A. C. W. van Rhijn, S. Postma, J. P. Korterik, J. L. Herek, and H. L. Offerhaus, *J. Opt. Soc. Am. B* **26**, 559 (2009).
- <sup>4</sup>W. Wöhlleben, T. Buckup, J. L. Herek, and M. Motzkus, *ChemPhysChem* **6**, 850 (2005).
- <sup>5</sup>P. Nuernberger, G. Vogt, T. Brixner, and G. Gerber, *Phys. Chem. Chem. Phys.* **9**, 2470 (2007).
- <sup>6</sup>S.-H. Shim and M. T. Zanni, *Phys. Chem. Chem. Phys.* **11**, 748 (2009).
- <sup>7</sup>A. M. Weiner, *Opt. Commun.* **284**, 3669 (2011).
- <sup>8</sup>E. Frumker and Y. Silberberg, *Opt. Lett.* **32**, 1384 (2007).
- <sup>9</sup>R. S. Pillai, C. Boudoux, G. Labroille, N. Olivier, I. Veilleux, E. Farge, M. Joffre, and E. Beaurepaire, *Opt. Express* **17**, 12741 (2009).
- <sup>10</sup>I. A. Walmsley, *Opt. Photon. News* **10**, 28 (1999).
- <sup>11</sup>We note that this particular LCD cannot achieve perfect phase-only modulation. More recent devices, such as the Holoeye PLUTO-NIR-2, can provide larger phase shifts with no amplitude leakage.
- <sup>12</sup>R. Trebino, K. W. DeLong, D. N. Fittinghoff, J. N. Sweetser, M. A. Krumbügel, B. A. Richman, and D. J. Kane, *Rev. Sci. Instrum.* **68**, 3277 (1997).